Effect of Pressure Fluctuation on Coal Combustion in Large-Particle Fluidized Beds

R. J. BYWATER
The Aerospace Corp.
Los Angeles, CA 90009

and

P. M. CHUNG
College of Engineering
University of Illinois
Chicago, IL 60680

Atmospheric fluidized-bed combustors (AFBC) operate in the large-particle (>1 mm) fluidization regime. Characteristics of this regime, combined with the fact that as much as 50% of the coal combustibles are volatiles, result in localization of the devolatilization and combustion of the volatilized gases to the neighborhood of the coal-particle and volatile gas plumes arising from the injector region. The volatile gas plume resulting from the large-particle fluidization dynamics wanders due to pressure fluctuations induced by bubble passage.

The purpose of the present work is to determine the impact of these characteristics on the design of AFBC's. This has been accomplished by a linearized analysis of the governing equations to describe the periodic wandering of the volatiles plume diffusion flame and the corresponding fluctuation of the combustion rate. The flame oscillation increases the overall combustion rate above the steady-state value. This increase diminishes with increasing fluctuation frequency until the flame becomes insensitive to the fluctuation in the high frequency limit.

SCOPE

Utility-scale atmospheric fluidized-bed combustors (AFBC) differ from other fluidized-bed applications in that the growth in size and speed of the bubbles are restricted by the large particles (~1 mm) that fill the bed and the immersed tubes. The beds, therefore, operate in either a slow bubble or a turbulent-churning flow regime. Park et al. (1979) proposed a "plume model" to analyze the coal combustion in the AFBC. In this plume model, the coal particles were assumed to devolatilize instantaneously upon entering the bed. The gaseous volatile matter then rose through the bed as a plume and burned as it mixed with oxygen. Since the kinetics of combustion between the gaseous volatile matter and oxygen are fast, Park et al.'s (1979) analysis consisted of that for a diffusion flame established between a jet of gaseous fuel and the surrounding oxygen.

The characteristic devolatilization time of the coal particles is known to be of the order of the coal circulation time (Field et al., 1967; Ubhayakar, et al., 1967); therefore, the instantaneous devolatilization assumption of Park et al. (1979) may not be accurate. Bywater (1980) included finite rate devolatilization kinetics in an injector region model and showed that often the finite rate kinetics become the controlling factor of combustion. It was further shown that finite rate effects coupled with solids dispersion can enhance volatiles escape. This phenomenon occurs when the volatiles are not completely consumed in the bed and escape into the free board where combustion proceeds at higher temperatures altering bed energetics and free-board heat transfer.

Experimental observations, such as those by Jovanovic (1979), show that the plumes in the fluidized beds wander and fluctuate driven by the pressure fluctuations expected in such system. The coal particles introduced at the injector devolatilize and mix with the surrounding char and chemically-inert particles that rise through the bed. The plume, therefore, wanders across an inhomogeneous solid-particle medium, and the wandering is expected to affect combustion.

The effect of the plume fluctuation (wandering) on the combustion of the volatile matter is studied in this paper within the context of the Park et al. (1979) and Bywater (1980) plume model. Such a study would test the accuracy of the steady-state solutions commonly employed for fluidized-bed combustors. Also, if it is found beneficial, this study may lead to future investigation of the possibility of producing a controlled pressure fluctuation in the combustors. To render the analysis tractable, a plane plume is considered, and the fluctuation is considered to be harmonic and small in amplitude. The governing equations are linearized and a closed form solution is obtained.

CONCLUSIONS AND SIGNIFICANCE

In the utility scale, atmospheric fluidized-bed coal combustors devolatilization and combustion of volatile gases are localized. The coal particles and the volatilized gas comprise plumes (rising jets) above the injector. The bubble-induced pressure fluctuations cause wandering of the gas plume and the flame. The effect of the fluctuation on the scale of flame wandering and, in turn, on the combustion rate was analyzed.

The pressure fluctuation was considered to engender a small harmonic periodic gas motion in the lateral direction. The resulting periodic wandering of the diffusion flame and the attendant fluctuation of the combustion rate were described by solving the governing equations in closed form.

The periodic motion of the flame and the variation of the combustion rate were found to be asymmetric with respect to the steady-state flame position and combustion rate. The fluctuation was found to result in an increased combustion rate from the steady-state value when integrated over a cycle. This increase diminished as the frequency of the pressure fluctuation increased. In the high frequency limit, the flame became insensitive to the fluctuation.

Existence of bubble-induced pressure fluctuations was known in atmospheric fluidized-bed coal combustors. The present

0001-1541-83-6814-0396-$2.00.

analysis showed that such fluctuations, which cause the flame to wander, could be beneficial to combustion. It may be useful in the future to investigate the possibility of producing controlled fluctuations in the fluidized-bed combustors.

Finally, to render the problem tractable, the fluctuations were considered to be small and the equations were linearized. Therefore, the numerical results obtained are expected to be inaccurate when the fluctuations are large. As with the most linearized theories, however, the qualitative aspects of the present findings should be still valid.

FORMULATION

The solid particulate constituent of the mixed medium, Figure 1, is comprised of coal, char, and limestone, while the volatile matter, oxygen, combustion products, and the chemically-inert gases comprise the gaseous constituent. The coal particles are considered to be introduced at $x = 0$ as a uniform plane jet of width 2ℓ. After Park et al. (1979) and Bywater (1980), we assume that the gaseous and the particulate species velocities are uniform and denoted by u_g and u_s, respectively.

As the coal particles rise with u_s, they devolatilize, with rate constant k_s, and engender the volatile gas plume. Both the coal particle and volatile gas jets diffuse laterally, as they rise in accordance with the turbulent diffusion coefficients D_s and D_g, respectively.

Consider now that a small pressure fluctuation associated with bubble movement in the bed causes a lateral, periodic motion of the fluid in the neighborhood of the plume as

$$v_g(x,t) = v_o(x) \cos \omega t. \tag{1}$$

Since the pressure and the attendant velocity fluctuations are small, we may consider that the steady flow and diffusion of the solid particles remain unaffected.

Governing Equations

Description of the problem requires the following conservation equations for concentrations of the volatile matter in the coal particles, C_s, and gaseous state, C_a, and for concentration of the oxygen, C_b.

$$u_s \frac{\partial C_s}{\partial x} = D_s \frac{\partial^2 C_s}{\partial y^2} - k_s C_s, \tag{2}$$

$$\frac{\partial C_a}{\partial t} + u_g \frac{\partial C_a}{\partial x} + v_g \frac{\partial C_a}{\partial y} = D_g \frac{\partial^2 C_a}{\partial y^2} + k_s C_s + W_a, \tag{3}$$

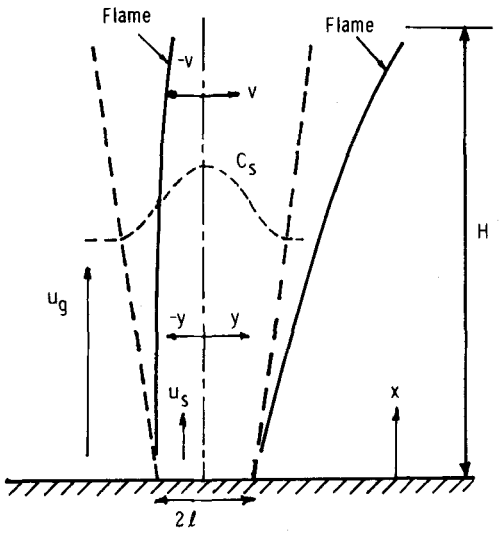

Figure 1. Sketch of volatile gas and solid particle plumes.

$$\frac{\partial C_b}{\partial t} + u_g \frac{\partial C_b}{\partial x} + v_g \frac{\partial C_b}{\partial y} = D_g \frac{\partial^2 C_b}{\partial y^2} + W_b. \tag{4}$$

In the above equations, the oxygen consumption by char combustion, included in Bywater's work (1980), is neglected, for it does not fundamentally alter the effect of fluid fluctuation on combustion of the volatile matter. Other than representing the two-dimensional jet configuration, the present equations differ from those employed by Bywater (1980) in that Eqs. 3 and 4 contain the unsteady terms and the terms with v_g. The gaseous combustion terms, w_a and w_b, are obtained by assuming the one-step reaction,

$$a(\text{fuel}) + b(\text{oxygen}) \xrightarrow{k_f} d(\text{product}), \tag{5}$$

as

$$w_a = -\frac{k_f}{\rho} \frac{a}{M_a^{a-1} M_b^b} C_a^a C_b^b, \tag{6}$$

and

$$w_b = \frac{bM_b}{aM_a} W_a. \tag{7}$$

Boundary conditions are specified for Eqs. 2–4 as follows. At $x = 0$:

$$\begin{aligned} C_s(0,y) &= C_{sp} \quad \text{for } -l \le y \le l, \\ &= 0 \quad \text{for } y < -l \text{ and } y > l \end{aligned} \tag{8}$$

$$C_a(0, y, t) = 0. \tag{9}$$

$$C_b(0,y,t) = C_{b\infty}. \tag{10}$$

At $y = \pm\infty$:

$$C_s(x,\pm\infty) = 0. \tag{11}$$

$$C_a(x,\pm\infty,t) = 0. \tag{12}$$

$$C_b(x,\pm\infty,t) = C_{b\infty}. \tag{13}$$

Nondimensionalization

With subsequent linearization and other conveniences in mind, we nondimensionalize the governing equations such that each term will be, at the most, of order one. Guided by the available chemically-reacting boundary layer work (Chung, 1965), we define the dimensionless variables,

$$\xi = x/H, \quad \eta = y\left(\frac{u_g}{D_g H}\right)^{1/2}, \quad \tau = tu_g/H,$$

$$L = l\left(\frac{u_g}{HD_g}\right)^{1/2}, \quad V = v_g\left(\frac{H}{D_g u_g}\right)^{1/2}, \quad \hat{D} = \frac{D_s u_g}{D_g u_s}. \tag{14}$$

$$\Gamma = \frac{k_s H}{u_s}, \quad \hat{C}_s = \left(\frac{bM_b}{aM_a}\right)\frac{C_s}{C_{b\infty}},$$

$$\hat{C}_a = \left(\frac{bM_b}{aM_a}\right)\frac{C_a}{C_{b\infty}}, \quad \hat{C}_b = \left(\frac{bM_b}{aM_a}\right)\frac{C_b}{C_{b\infty}}. \tag{15}$$

Equations 2–4 are then put into the following nondimensional form with the use of Eqs. 6, 7, 14 and 15.

$$\frac{\partial \hat{C}_s}{\partial \xi} = \hat{D}\frac{\partial^2 \hat{C}_s}{\partial \eta^2} - \Gamma \hat{C}_s, \tag{16}$$

$$\frac{\partial \hat{C}_a}{\partial \tau} + \frac{\partial \hat{C}_a}{\partial \xi} + V\frac{\partial \hat{C}_a}{\partial \eta} = \frac{\partial^2 \hat{C}_a}{\partial \eta^2} + \left(\frac{u_s}{u_g}\right)\Gamma \hat{C}_s - \left(\frac{a}{M_a^{a-1}M_b^b}\right)\left(\frac{aM_a}{bM_b}C_{b\infty}\right)^{a+b-1}\frac{H}{u_g}\frac{k_f}{\rho}\hat{C}_a^a\hat{C}_b^b, \quad (17)$$

$$\frac{\partial \hat{C}_b}{\partial \tau} + \frac{\partial \hat{C}_b}{\partial \xi} + V\frac{\partial \hat{C}_b}{\partial \eta} = \frac{\partial^2 \hat{C}_b}{\partial \eta^2} - \left(\frac{bM_b}{aM_a}\right)\left(\frac{a}{M_a^{a-1}M_b^b}\right)\left(\frac{aM_a}{bM_b}C_{b\infty}\right)^{a+b-1}\frac{H}{u_g}\frac{k_f}{\rho}\hat{C}_a^a\hat{C}_b^b. \quad (18)$$

Reduction of Eqs. 17 and 18

The coefficient of $\hat{C}_a^a\hat{C}_b^b$ in Eqs. 17 and 18 is the Damkohler number for combustion of the volatile gas (Chung, 1965). It is the ratio of the characteristic residence time of the reactants to the characteristic chemical reaction time.

Consider the limit of a large Damkohler number,

$$\left(\frac{a}{M_a^{a-1}M_b^b}\right)\left(\frac{aM_a}{bM_b}C_{b\infty}\right)^{a+b-1}\frac{H}{u_g}\frac{k_f}{\rho} \to \infty, \quad (19)$$

which is obtained in the fluidized bed of the present interest (Park, et al., 1979; Bywater, 1980).

Since each term of Eqs. 17 and 18 are at the most of order one, the condition of Eq. 19 demands that

$$\hat{C}_a^a\hat{C}_b^b = 0. \quad (20)$$

Equation 20 is the condition for existence of a diffusion flame in the limit shown in Eq. 19.

Equations 17 and 18 are combined to eliminate the last terms, as,

$$\frac{\partial m}{\partial \tau} + \frac{\partial m}{\partial \xi} + V\frac{\partial m}{\partial \eta} = \frac{\partial^2 m}{\partial \eta^2} + \left(\frac{u_s}{u_g}\right)\Gamma \hat{C}_s, \quad (21)$$

where

$$m = \hat{C}_a - \frac{aM_a}{bM_b}\hat{C}_b. \quad (22)$$

We have now reduced Equations (17) and (18) to a much simpler pair of equations—Eqs. 20 and 21. Equation 16 is unaffected.

We complete the formulation by transforming the boundary conditions, Eqs. 8–13, to those for Eqs. 16 and 21 as follows.

At $\xi = 0$:

$$\hat{C}_s(0,\eta) = \hat{C}_{sp} \quad \text{for } -L \le \eta \le L, \qquad = 0 \quad \text{for } \eta < -L \text{ and } \eta > L \quad (23)$$

$$m(0,\eta,\tau) = -1. \quad (24)$$

For $\eta \to \pm\infty$:

$$\hat{C}_s(\xi,\pm\infty) = 0. \quad (25)$$

$$m(\xi,\pm\infty,\tau) = -1. \quad (26)$$

ANALYSIS

Complex Plane

We seek the solution of Eqs. 16, 21 and 20 satisfying the boundary conditions, Eqs. 23–26, and the oscillatory motion, Eq. 1. Following the standard approach, we go to the complex plane and rewrite Eq. 1 as,

$$V(\xi,\tau) = V_o(\xi)e^{i\Omega\tau}, \quad (27)$$

where

$$V_o = v_o\left(\frac{H}{D_g u_g}\right)^{1/2}, \quad (28)$$

and

$$\Omega = \frac{H}{u_g}\omega.$$

A solution is sought for the small fluctuation (wandering) velocity,

$$V_o \ll 1. \quad (29)$$

In view of Eqs. 27 and 29, we construct the solution in the form,

$$\hat{C}_a(\xi,\eta,\tau) = \hat{C}_{ao}(\xi,\eta) + \beta(\xi,\eta)e^{i\Omega\tau},$$
$$\hat{C}_b(\xi,\eta,\tau) = \hat{C}_{bo}(\xi,\eta) + \gamma(\xi,\eta)e^{i\Omega\tau}, \quad (30)$$
$$m(\xi,\eta,\tau) = m_o(\xi,\eta) + \alpha(\xi,\eta)e^{i\Omega\tau},$$

where $\hat{C}_{ao}$, $\hat{C}_{bo}$, and m_o, and β, γ, and α are related through Eq. 22, and

$$\frac{\alpha}{m_o}, \quad \frac{\beta}{\hat{C}_{ao}}, \quad \frac{\gamma}{\hat{C}_{bo}} \ll 1. \quad (31)$$

A substitution of Eqs. 27 and 30 into Eq. 21 results in the following two equations when the terms of order of magnitude smaller than one are neglected.

$$\frac{\partial m_o}{\partial \xi} = \frac{\partial^2 m_0}{\partial \eta^2} + \left(\frac{u_s}{u_g}\right)\Gamma \hat{C}_s, \quad (32)$$

$$i\Omega\alpha + \frac{\partial \alpha}{\partial \xi} + V_o\frac{dm_o}{d\eta} = \frac{\partial^2 \alpha}{\partial \eta^2}. \quad (33)$$

Boundary conditions for the above equations are obtained from Eqs. 24 and 26 as

At $\xi = 0$:

$$m_o(0,\eta) = -1, \quad (34)$$

$$\alpha(0,\eta) = 0. \quad (35)$$

For $\eta \to \pm\infty$:

$$m_o(\xi,\pm\infty) = -1, \quad (36)$$

$$\alpha(\xi,\pm\infty) = 0. \quad (37)$$

Solution of Eqs. 16 and 32

A Green's function (Jakob, 1955; Ozisik, 1968) can be readily constructed for Eq. 16 to satisfy the boundary conditions 23 and 25. A manipulation of the function results in the solution,

$$\hat{C}_s(\xi,\eta) = \frac{\hat{C}_{sp}}{2}\exp(-\Gamma\xi) \times \left\{\text{erf}\left[\frac{\eta + L}{2(\hat{D}\xi)^{1/2}}\right] - \text{erf}\left[\frac{\eta - L}{2(\hat{D}\xi)^{1/2}}\right]\right\}. \quad (38)$$

Consider now Eq. 32. The variable, $\hat{C}_s$, given by Eq. 38 and the boundary conditions, Eqs. 34 and 36, are all real. Therefore, m_o is expected to be real also. Using Eq. 38 for $\hat{C}_s$, a Green's function satisfying Eqs. 34 and 36 is constructed for m_o. After some manipulation, the Green's function gives the solution,

$$m_o(\xi,\eta) = -1 + \frac{\hat{C}_{sp}}{2}\frac{u_s}{u_g}\Xi \times \int_0^\xi \exp(-\Gamma\xi')\left[\text{erf}\frac{(\eta + L)}{2(\hat{D}\xi' - \xi' + \xi)^{1/2}} - \text{erf}\frac{(\eta - L)}{2(\hat{D}\xi' - \xi' + \xi)^{1/2}}\right]d\xi'. \quad (39)$$

When $\hat{D} = 1$, this equation reduces to

$$m_o(\xi,\eta) = -1 + \frac{\hat{C}_{sp}}{2}\frac{u_s}{u_g}\left[\text{erf}\left(\frac{\eta + L}{2\xi^{1/2}}\right) - \text{erf}\left(\frac{\eta - L}{2\xi^{1/2}}\right)\right][1 - \exp(-\Gamma\xi)]. \quad (40)$$

Solution of Eq. 33

Clearly, Eq. 33 is complex and its closed-form general solution is not readily obtainable. With a series solution in mind, let us first investigate the magnitude of Ω for cases of interest. It is more likely that the gas fluctuation will complete one or more cycles during the gas residence time in the bed. This means that

$$\frac{2\pi}{\omega} \leq \frac{H}{u_g}, \tag{41}$$

which can be rewritten as,

$$\Omega \geq 2\pi. \tag{42}$$

We, therefore, will construct a series solution of Eq. 33 valid for large values of Ω.

We write,

$$\alpha(\xi,\eta,\Omega) = \frac{1}{(i\Omega)}\delta_o(\xi,\eta) + \frac{1}{(i\Omega)^2}\delta_1(\xi,\eta) + 0\left(\frac{1}{i\Omega}\right)^3. \tag{43}$$

The symbol o denotes the order of magnitude of the term (Van Dyke, 1965). A substitution of Eq. 43 into Eq. 33 generates the following equations for δ_o and δ_1.

$$\delta_o = -V_o\frac{\partial m_o}{\partial \eta}, \tag{44}$$

$$\delta_1 = \frac{\partial^2\delta_o}{\partial\eta^2} - \frac{\partial\delta_o}{\partial\xi}. \tag{45}$$

In order for α to satisfy the boundary conditions, Eqs. 35 and 37, both δ_o and δ_1 must satisfy the zero boundary conditions at $\xi = 0$ and $\eta = \pm\infty$. Equations 44 and 45 are algebraic expressions since m_o is given by Eq. 39. However, these expressions automatically satisfy the zero boundary conditions since all derivatives of m_o vanish at $\xi = 0$ and $\eta = \pm\infty$. Therefore, there is no singular region in the limit of $\Omega \to \infty$ in contrast to the related problems analyzed by Lighthill (1954) and Chung (1969). Consequently, the solutions given by Eqs. 43–45 are uniformly valid (Van Dyke, 1965).

Results

The solution of Eq. 16 for $\hat{C}_s$ is given by Eq. 38.

Equations 17 and 18 for the diffusion flame and Eq. 19, are combined into an equivalent set, Eqs. 20–22. The solution of Eq. 21 is constructed from Eqs. 30, 43, 44 and 45 for order up to $1/(i\Omega)^3$ as,

$$m(\xi,\eta,\tau) = m_o(\xi,\eta) + i\frac{V_o}{\Omega}\left[\frac{\partial m_o}{\partial\eta} + \frac{1}{i\Omega}\left(\frac{\partial^3 m_o}{\partial\eta^3} - \frac{\partial^2 m_o}{\partial\xi\partial\eta}\right)\right]e^{i\Omega\tau}. \tag{46}$$

The real part of m is

$$R\{m\} = m_o - \frac{V_o}{\Omega}\left[\frac{\partial m_o}{\partial\eta}(\sin\Omega\tau) + \frac{1}{\Omega}\left(\frac{\partial^2 m_o}{\partial\xi\partial\eta} - \frac{\partial^3 m_o}{\partial\eta^3}\right)(\cos\Omega\tau)\right], \tag{47}$$

where the function m_o is given by Eq. 39, and the derivatives are obained from differentiation of that equation.

Equations 20 and 22 together with the boundary conditions, Eqs. 9, 10, 12 and 13, dictate the following structure of the diffusion flame.

The position of the flame, η^*, is defined by the implicit equation

$$R\{m(\eta^*)\} = 0. \tag{48}$$

For $\eta \leq \eta^*$,

$$R\{\hat{C}_b\} = 0, \tag{49}$$

and

$$R\{\hat{C}_a\} = R\{m\}. \tag{50}$$

For $\eta \geq \eta^*$,

$$R\{\hat{C}_a\} = 0, \tag{51}$$

and

$$R\{\hat{C}_b\} = -\frac{bM_b}{aM_a}R\{m\}. \tag{52}$$

Combustion rate per half of the plume for a given ξ and τ is given by the equation,

$$I_a = -\frac{bM_b}{aM_a}\frac{1}{C_{b\infty}}\left(\frac{H}{u_g D_g}\right)^{1/2}\int_0^\infty W_a dy = -R\left\{\left(\frac{\partial m}{\partial\eta}\right)_{\eta^*}\right\} + \frac{u_s}{u_g}\Gamma\int_{\eta^*}^\infty \hat{C}_s d\eta. \tag{53}$$

The flame position, η^*, is determined from Eqs. 47 and 48 numerically. $R\{(\partial m/\partial\eta)_{\eta^*}\}$ for Eq. 53 is then obtained by differentiating Eq. 47.

DISCUSSION

If we consider a typical fluidized combustor environment wherein $H \sim 1$ m, $D_g \sim 1$ cm^2/s, and $u_g \sim 1$ m/s, and if we assume $\hat{D} \sim 1$, $u_g H/D_g$ is of the order of 10^4. The initial coal jet width of 8 cm than corresponds to $L \sim 4$.

Figures 2 through 6 show typical variations with respect to the time of the flame position and combustion rate for a given upward position ξ and set of governing parameters. The fluctuation of V which causes the flame wandering is also shown.

The following observations are common to all cases shown. The flame wanders deeper into the coal particle-jet side than into the opposite side of the steady state position, η_o^*. The unsteady instantaneous combustion rate is greater than the steady-state combustion rate when the flame is on the particle-jet side of the steady-state flame position. On the other hand, the reverse is true when the flame is on the other side of the steady-state flame position. These excesses and deficits of the combustion rate do not

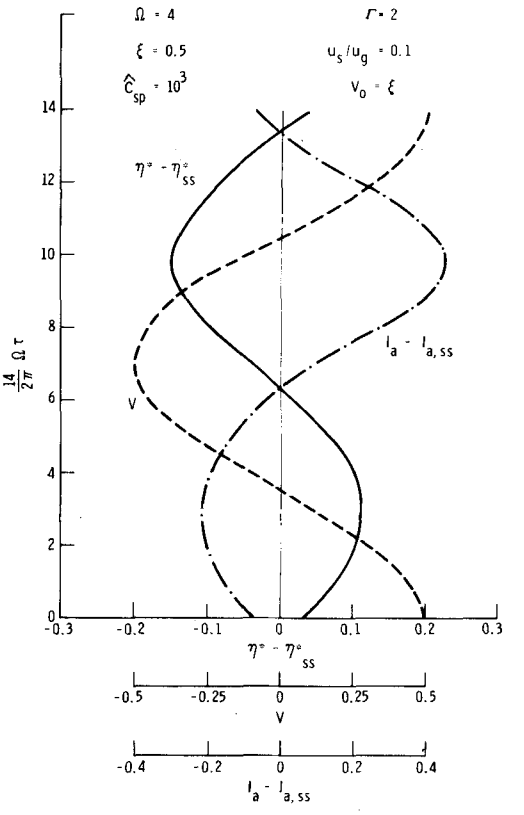

Figure 2. Fluctuation of flame position and combustion rate.

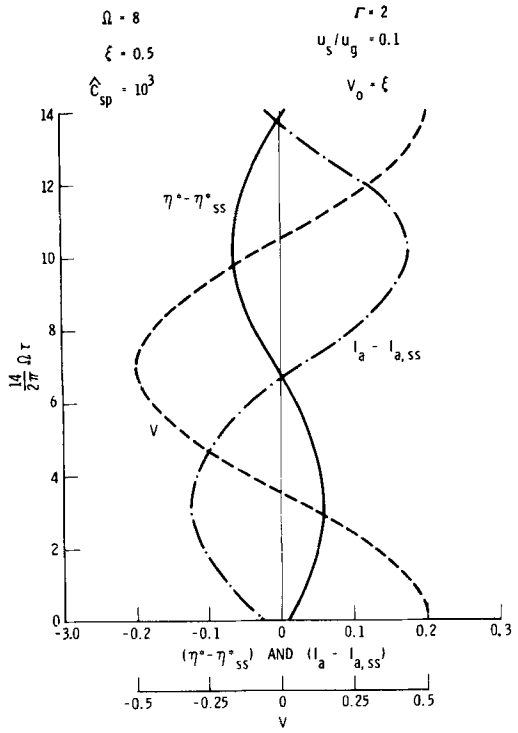

Figure 3. Fluctuation of flame position and combustion rate.

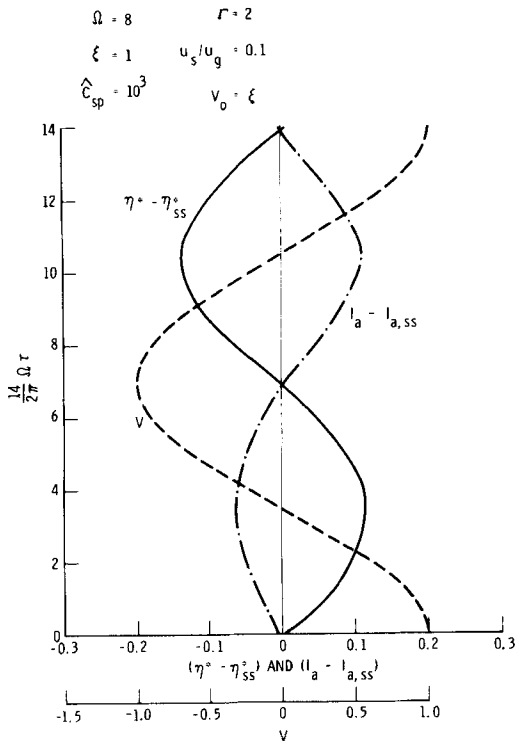

Figure 4. Fluctuation of flame position and combustion rate.

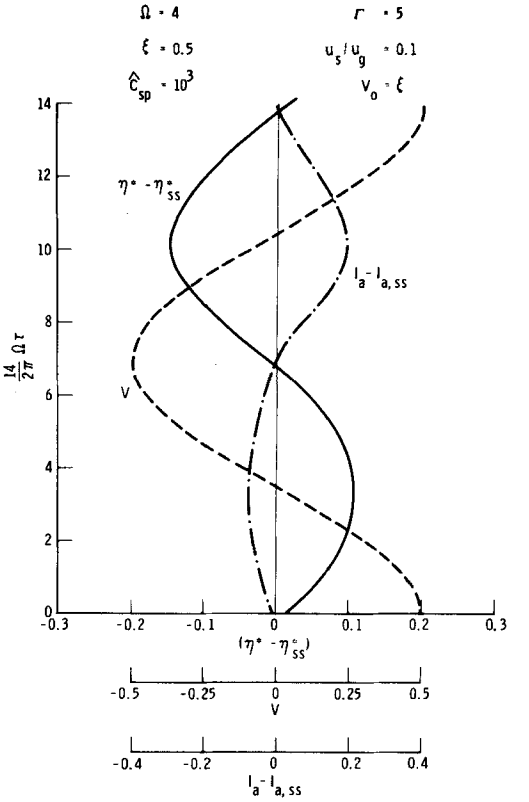

Figure 5. Fluctuation of flame position and combustion rate.

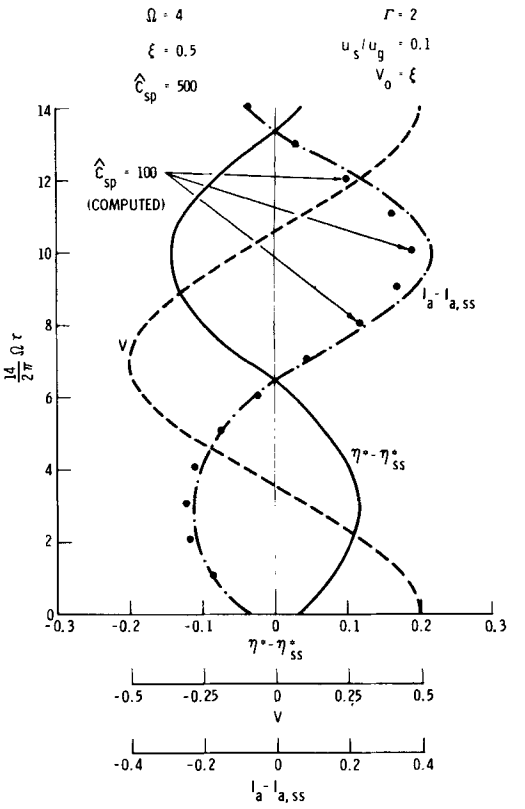

Figure 6. Fluctuation of flame position and combustion rate.

cancel, and there is a net increase in the combustion rate for a cycle over the steady state value. Therefore, the periodic wandering of the flame caused by pressure fluctuation results in an enhanced combustion of volatiles.

A comparison of Figures 2 and 3 shows that as Ω increases, the flame oscillation becomes more sinusoidal in form accompanied by decreasing amplitude. With a continuous increase in Ω, the flame becomes oblivious to the V fluctuation. Also, when the Ω was doubled from 4 to 8, the increase in the one-cycle combustion rate over the steady-state value is more than halved. For a given period of time, there are twice as many cycles when $\Omega = 8$ than when $\Omega = 4$. Therefore, for a given amplitude of V-variation, smaller oscillation frequency results in a greater enhancement of combustion rate in the range of $\Omega \geq 2\pi$.

Figures 3 and 4 show that, at a further downstream location, the larger amplitude of V-variation causes a greater amplitude of the

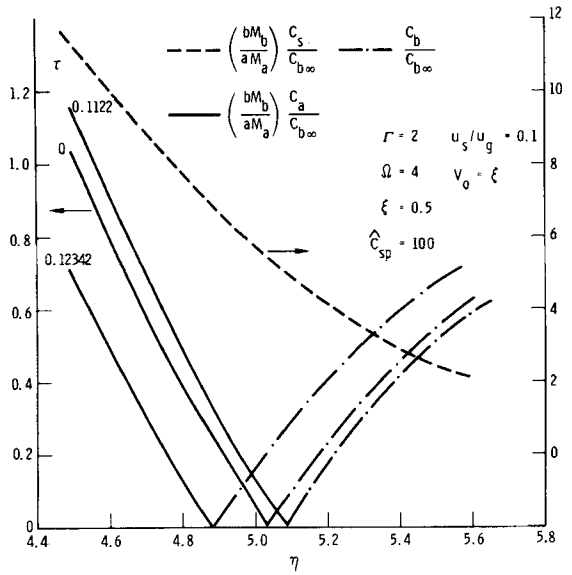

Figure 7. Fluctuation of volatile gas and oxygen concentrations.

flame fluctuation. Amplitude of the combustion rate variation, however, is reduced since C_s is depleted.

A comparison of Figures 2 and 5 shows that the greater Damkohler number, Γ, has little effect on the flame fluctuation. On the other hand, the amplitude of the combustion rate variations is reduced. This is because, for a given ξ, a greater Γ implies a greater depletion of C_s upstream.

A comparison of Figures 2 and 6 shows that the magnitude of $C_{sp}/C_{b\infty}$ has a small effect on the flame and combustion rate fluctuations. Figure 6 contains the combustion rate fluctuations. Figure 6 contains the combustion rate fluctuations for $C_{sp}/C_{b\infty}$ of 500 and 100. They differ very little from each other. The flame fluctuations were found to be even closer to each other than the combustion rate fluctuations.

Variations with respect to time of the C_a and C_b profiles are shown on Figure 7. The invariant C_s profile is also shown. The flame fluctuates across the nonuniform C_s distribution, and this results in the asymmetric variation of the combustion rate and, consequently, in the net increase of combustion rate over the steady-state value.

NOTATION

a = stoichiometric coefficient for volatile gas
b = stoichiometric coefficient for oxygen
C = concentration, kg/m^3
$\hat{C}$ = normalized concentration defined in Eqs. 15
D = turbulent diffusivity, m^2/s
$\hat{D}$ = parameter defined in Eqs. 14
d = stoichiometric coefficient for combustion product
H = bed height, m
Ia = dimensionless combustion rate defined by Eq. 53
k_f = rate constant for combustion reaction of Eq. 5, $\frac{\text{kg}\cdot\text{m}^{3(a+b-2)}}{(\text{mol})^{a+b-1}\text{s}}$
k_s = rate constant for devolatilization, L/s
L = normalized injector half width defined in Eq. 14
ℓ = injector half width, m
M = molecular weight, kg/mol
m = normalized function defined by Eq. 22
$R\{\ \}$ = real part
t = time, s
u = upward stream velocity, m/s
V = normalized lateral velocity defined by Eq. 14
V_o = normalized amplitude of lateral velocity oscillation defined by Eq. 27
v = lateral velocity, m/s
v_o = amplitude of lateral velocity oscillation, m/s
W = production rate by combustion, kg/m^3·s
x = upward distance, m
y = lateral distance, m

Greek Letters

α,β,γ = functions defined by Eqs. 30
δ = functions defined by Eq. 43
η = normalized variable defined by Eqs. 14
ξ = normalized variable defined by Eqs. 14
ρ = gas density, kg/m^3
τ = normalized time defined by Eqs. 14
Ω = normalized frequency defined by Eqs. 28
ω = lateral velocity oscillation frequency defined by Eq. 1, L/s

Subscripts

a = volatile gas
b = oxygen
g = gas
o = zeroth-order terms defined in Eqs. 30
p = evaluated at the injector
s = solid particles in general, and volatile matter contained in solid particles for C_s
ss = steady state
∞ = evaluated at far from the plumes

LITERATURE CITED

Bywater, R. J., "The Effects of Devolatilization Kinetics on the Injector Region of Fluidized Beds," 6th International Conference on Fluidized Bed Combustion, Atlanta (April, 1980).

Chung, P. M., "Nonequilibrium Chemically Reacting Boundary Layers," *Advances in Heat Transfer*, **2**, Chapt. 2 (1965).

Chung, P. M., "Periodic Fluctuation of Chemical species over a Reactive Surface," *Phys. of Fluids*, **12**, 53 (1969).

Field, M., D. Gill, B. Morgan, and P. Hawksley, *Combustion of Pulverized Coal*, The British Coal Utilization Research Assoc., Leatherheat, England (1967).

Jakob, M., *Heat Transfer*, Wiley and Sons, Chapt. 15 (1955).

Jovanovic, G., Ph.D. Thesis, Oregon State University (1979).

Lighthill, M. J., "The Response of Laminar Skin Friction and Heat Transfer to Fluctuations in the Stream Velocity," Proc. Royal Soc., London, **A224**, 1 (1954).

Ozisik, M., *Boundary Value Problems of Heat Conduction*, International Textbook Co., Scranton, PA (1968).

Park, D., O. Levenspiel, and T. J. Fitzgerald, "A Model for Large Scale Atmospheric Fluidized Bed Combustors," AIChE Preprint No. 26C, Annual AIChE meeting, San Francisco (Nov., 1979).

Ubhayakar, S., D. Stickler, C. Von Rosenberg, Jr., and R. Cannon, "Rapid Devolatilization of Pulverized Coal in Hot Combustion Gases," Proc. 16th Symposium (International) on Combustion, MIT, Cambridge (Aug., 1976).

Van Dyke, M. D., *Perturbation Methods in Fluid Mechanics*, Academic Press, New York (1965).

Manuscript received November 5, 1981; revision received May 7, and accepted May 28, 1972.